Supporting Information

Hilge et al. 10.1073/pnas.0902171106

SI Text

ITC Data Analysis. With the exception of constructs binding a single Ca^{2+} ion, all data were analyzed with the "sequential binding sites model" implemented in the Origin 7.0 software (Microcal). This model accounts for the nonindependence of the individual Ca^{2+}-binding events and suggests the number of binding sites before the fitting. Constructs were measured at least three times to determine the optimal experimental conditions with respect to signal-to-noise ratio and the number of data points. In all cases, experiments were consistent and reproducible. All ITC data, displayed in Fig. 2 *A*, *C*, and *D*, Fig. S3, and Fig. S5, are the result of a single ITC experiment under the determined conditions. Protein concentrations were generally 80 μM, except for Ca^{2+} titrations of NCX2 CBD2 (Fig. 2*C* and Fig. S3*D*), NCX3 CBD2-B (Fig. 2*C* and Fig. S3*F*), and NCX3 CBD2 E578D/E585K (Fig. S3*H*) where we used 200 μM protein samples to overcome low signal-to-noise ratios as a consequence of small heat pulses. Endothermic heat pulses, absent at lower protein concentrations, were accounted for by the inclusion of an artificial Ca^{2+}-binding site that refined to K_d values of 100 μM–1 mM.

Particle-Induced X-Ray Emission (PIXE) Analysis. To determine the exact stoichiometry of the Ca^{2+} ions present in the CBD12-AD and CBD12-ACDEF constructs, we used PIXE analysis, where a strong proton beam induces X-ray fluorescence characteristic for the elements present in the sample. In proteins of known sequence the number of sulfurs can be used as an internal calibration. As a prerequisite, sodium and chloride ions had to be removed from the sample (both give overlapping X-ray emission signals with sulfur) and any other source of sulfur than the protein. Hence, the generally used protein buffer (30 mM NaCl, 130 mM KCl, 2.5 mM β-mercaptoethanol, and 1 mM Hepes, pH 7.0) was exchanged for a 160 mM KBr, 1 mM Bis-Tris propane, pH 7.0, buffer using a 10-kDa amicon ultra filter device (Millipore). The calcium-to-sulfur ratios were then determined with 2.5 MeV proton microbeam PIXE at the Surrey Ion Beam Centre using the method of Garman and Grime (1).

SAXS Data Analysis. We initially calculated in a model-independent approach for each construct and condition 20 ab initio reconstructions with the program GASBOR (2). We then compared the reconstructions by superposition. Applying a normalized spatial discrepancy (NSD) selection criterion, at most 1 of 20 structures were rejected. Averaging of the remaining structures with the program DAMAVER (3) resulted in a representative beads model (Fig. 4). Likewise for the rigid-body modeling approach, 20 calculations for each construct and condition were performed with the program SASREF (4). For this purpose, scattering profiles of 20 combinations of individual, lowest-energy CBD1 and CBD2-AD NMR structures were derived with the help of the program CRYSOL (5).

1. Garman EF, Grime GW (2005) Elemental analysis of proteins by microPIXE. *Prog Biophys Mol Biol* 89:173–205.
2. Svergun DI, Petoukhov MV, Koch MH (2001) Determination of domain structure of proteins from X-ray solution scattering. *Biophys J* 80:2946–2953.
3. Volkov VV, Svergun DI (2003) Uniqueness of ab initio shape determination in small-angle scattering. *J Appl Cryst* 36:860–864.
4. Petoukhov MV, Svergun DI (2005) Global rigid body modeling of macromolecular complexes against small-angle scattering data. *Biophys J* 89:1237–1250.
5. Svergun DI, Barberato C, Koch MHJ (1995) CRYSOL - a program to evaluate X-ray solution scattering of biological macromolecules from atomic coordinates. *J Appl Cryst* 28:768–773.
6. Hilge, M, Aelen, J, Vuister, GW (2006) Ca^{2+} regulation in the Na^{+}/Ca^{2+} exchanger involves two markedly different Ca^{2+} sensors. *Mol Cell* 22:15–25.

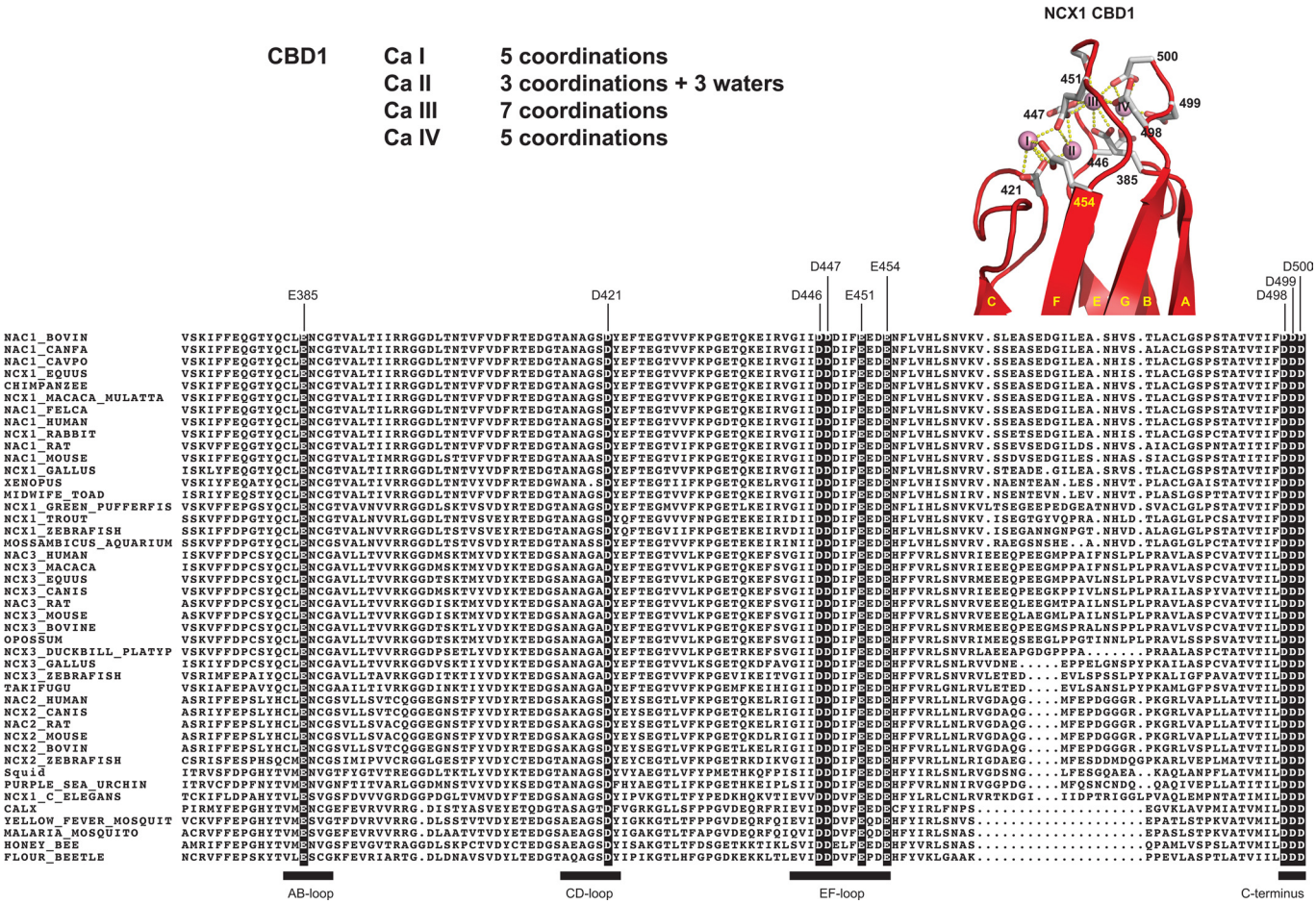

Fig. S1. Alignment of all available CBD1 sequences reveals strict conservation of the Ca^{2+} coordinating residues Glu-385, Asp-421, Asp-446, Asp-447, Glu-451, Glu-454, Asp-498, Asp-499, and Asp-500 as well as a generally high conservation of the AB-, CD-, and EF-loops, and the C terminus, where the Ca^{2+}-coordinating residues are located.

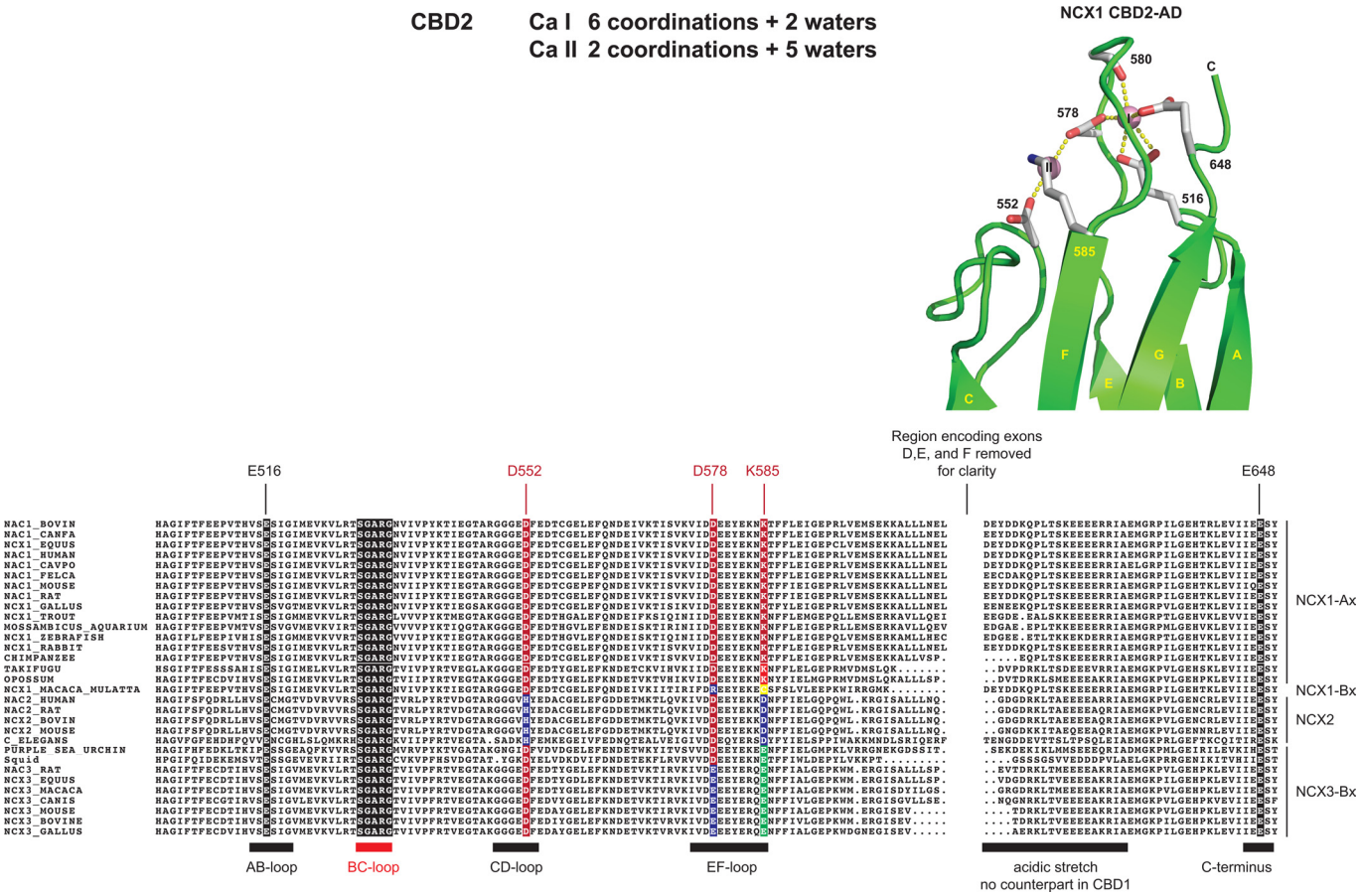

Fig. S2. Alignment of all available CBD2 sequences reveals strict conservation of Glu-516 and Glu-648 that contribute four of the six Ca^{2+} coordinating atoms in Ca^{2+}-binding site I of NCX1 CBD2-AD. In strong contrast, Ca^{2+}-binding site II displays isoform- and splice variant-specific variability in key-positions 552, 578, and 585. Rhesus monkey (*Macaca mulatta*) represents an exon B-containing NCX1 splice variant. In NCX2 isoforms and *C. elegans* positions 552 and 585 are occupied by a histidine and an aspartate residue, respectively. NCX3 sequences contain exon B and largely retain the Ca^{2+}-coordinating residues of CBD1. Indicated in red is the strictly conserved BC-loop that is located in the hinge between CBD1 and CBD2.

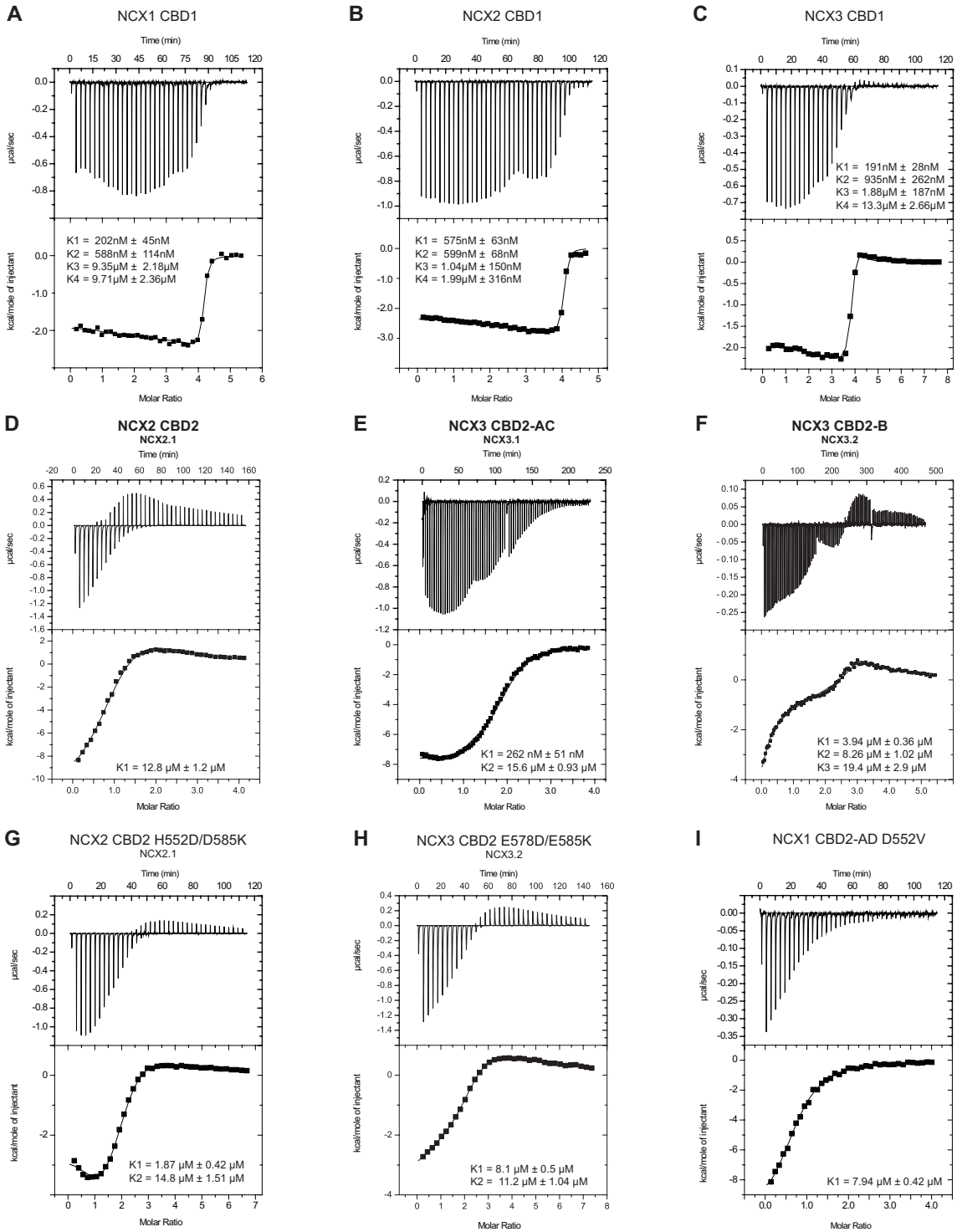

Fig. S3. Thermodynamic analyses of CBD1 and CBD2 and ITC control experiments of isoforms NCX2 and NCX3, designed to restore the Ca^{2+} coordination scheme of NCX1 CBD2-AD. ITC curves of NCX1 (*A*), NCX2 (*B*), and NCX3 (*C*) CBD1, obtained at pH 7 in 30 mM NaCl and 130 mM KCl, reveal only approximate affinity ranges and are very similar for the three isoforms. In contrast, binding isotherms of NCX2 CBD2 (*D*), NCX3 CBD2-AC (*E*), and NCX3 CBD2-B (*F*) suggest binding of one, two, and three Ca^{2+} ions, respectively. The NCX2 CBD2 H552D/D585K (*G*) and NCX3 E578D/E585K (*H*) double mutants reveal binding of 2 Ca^{2+} ions with macroscopic binding constants comparable to NCX1 CBD2-AD (1 and 9 μM) (6). Similarly to WT NCX2, the NCX1 CBD2-AD D552V mutant (*I*) shows binding of a single Ca^{2+} ion with relatively low affinity. Because of small heat pulses Ca^{2+} titrations of NCX2 CBD2 (Fig. S3*D*) and NCX3 CBD2-B (Fig. S3*F*) had to be performed at higher protein concentrations (200 μM). The endothermic heat pulses, absent at lower protein concentrations, were accounted for by including an additional Ca^{2+}-binding site that refined to K_d values of 100 μM or lower.

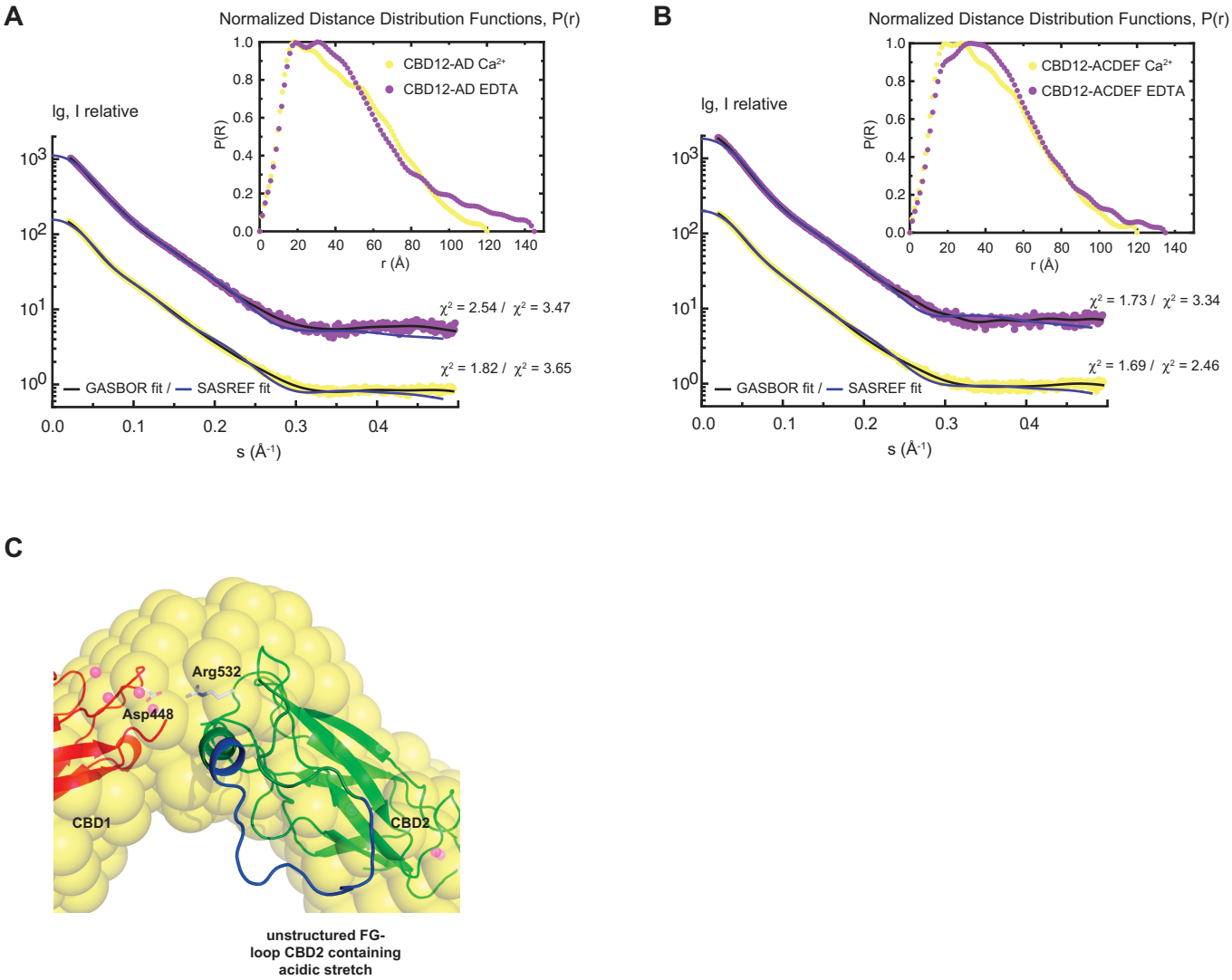

Fig. S4. SAXS scattering curves and normalized distance distribution functions P(r) of brain CBD12-AD (*A*) and heart CBD12-ACDEF (*B*) in the presence and absence of Ca^{2+}. (*C*) Hinge region between CBD1 and CBD2, displaying the acidic stretch (blue) in the unstructured FG-loop of CBD2 as well as the mutation-sensitive Asp-448 facing Arg-532 in the strictly conserved BC-loop of CBD2.

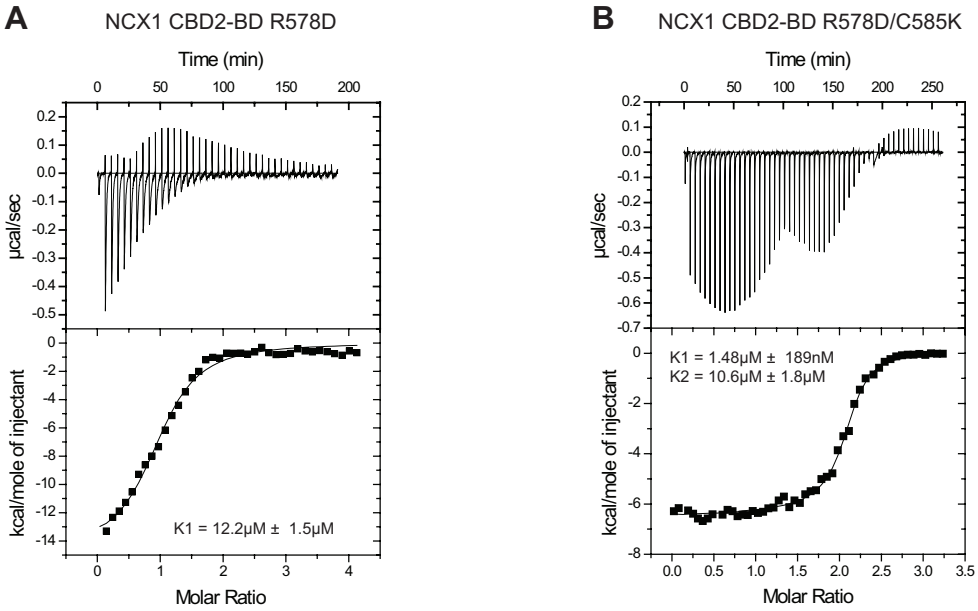

Fig. S5. Ca^{2+} titrations of the R578D and R578D/C585K CBD2-BD mutants for which functional data display modest and reestablished outward Na^{+}/Ca^{2+} exchange currents compared with NCX1.3. The ITC analyses of R578D and R578D/C585K reveal binding of one and two Ca^{2+} ions, respectively, as well as for the latter very similar Ca^{2+}-binding constants to CBD2-AD (6).

Table S1. Experimental NMR data and structural statistics for Ca^{2+} free CBD2-AD and CBD2-BD*

	CBD2-AD Ca^{2+} free	CBD2-BD
NOE upper distance limits		
Total	2,623	2,324
Long-range, spanning five or more residues	1,288	1,031
Distance constraint violations		
Total number >0.3 Å	0	0
rmsd	0.012 ± 0.001	0.012 ± 0.001
TALOS-derived angle constraints	145	140
rmsd	0.24 ± 0.06	0.37 ± 0.07
Violations >3°	2	3
PROCHECK† Ramachandran plot analysis		
Residues in favored regions	91.4%‡	91.1%§
Residues in additionally allowed regions	8.5%‡	8.5%§
Residues in generously allowed regions	0.1%‡	0.2%§
Residues in disallowed regions	0.1%‡	0.1%§
CING ROG-scores¶	20/39/41%	18/37/46%
rmsd to the averaged coordinates		
N, Cα, C′	0.43 ± 0.06 Å‡	0.46 ± 0.08 Å§
All heavy atoms	0.89 ± 0.08 Å‡	0.95 ± 0.10 Å§

*Average over the 20 conformers with the lowest NOE energies.
†Laskowski RA, Rullmannn JA, MacArthur MW, Kaptein R, Thornton JM (1996) AQUA and PROCHECK-NMR: programs for checking the quality of protein structures solved by NMR. *J Biomol NMR* 8:477–486.
‡Residues 502–577, 583–598, and 633–648.
§Residues 503–576, 586–597, 633–644.
¶http://proteins.dyndns.org/CING.